

Optimum Image Resolution of a micro-CT image to characterize shape descriptors of unconsolidated sand

Zubair Ahmed*

*Department of Exploration Geophysics
Curtin University, 26 Dick Perry Ave
Kensington, 6151 WA and
DET CRC, Australia
Zubair.ahmed1@postgrad.curtin.edu.au*

Maxim Lebedev

*Department of Exploration Geophysics
Curtin University, 26 Dick Perry Ave
Kensington, 6151 WA and
DET CRC, Australia
M.lebedev@curtin.edu.au*

SUMMARY

Resolution plays a fundamental role in any quantitative image analysis. Higher resolution images contain more details for further analysis but trade-off encounters when resultant smaller sample size raised question on representativeness of the whole sample. Image acquisition time and cost are also major issues that high resolution images have to face. To identify maximum image resolution that can avoid these issues as well as can provide accurate results in calculating shape factors, we study images of quartz sand grains acquired with four different resolutions. We present a comprehensive processing technique that can effectively extract individual grains from a 3D micro-CT image. Then we calculate equivalent diameter, volume and surface area of the grains at different resolutions. For all four resolutions, volume of grains shows very little change in lower two resolutions and almost no change through higher three resolutions, minimum of which can be considered as optimum. On the other hand, surface area for all the grains shows increasing trend with increasing resolution, but different in gradient. This different increasing trend can be explained by the surface rugosities and whether the image resolution can be able to resolve those. The higher two resolutions can effectively resolve surface irregularities of most of the grains, which is evident by their similar values of calculated surface areas. Therefore, minimum of these two resolutions can be considered as optimum image resolution in calculating shape factors for the studied grains.

INTRODUCTION

In unconsolidated sand; grain size, shape and sorting play crucial roles in terms of effective mechanical properties (Cavarretta 2009, Dondi et al. 2012, Ha Giang et al. 2015, Santamarina and Cho 2004). Recent advancement in micro-CT image acquisition (Wildenschild and Sheppard 2013) and uses of high speed computing facilities (Druckrey et al. 2016) with sophisticated processing techniques have excelled 3D grain shape visualization and quantification (Alshibli et al. 2015) over analysing 2D images (e.g. Cox and Budhu (2008)). Working with 3D images require a voxel based analysis where size of the voxel in input image should be small enough to capture the details of the grain surface. Đuriš et al. (2016) examined shape factors of quartz sand grains using different scanning resolutions in 2D images. Kröner and Doménech Carbó (2013) proposed a validation technique which lead to find the minimum pixel resolution for analysing shape factors in 2D images. Bazaikin et al. (2017) showed a systematic analysis of the effect of micro-CT image size and resolution on estimation of porosity, specific surface area, mean curvature, and topology of the pore space.

High resolution images obviously provide more detailed analysis and accurate shape factors. But such images restrict the sample size small which sometimes limits the representativeness of the heterogeneous samples. Moreover, acquisition and processing those images are often time consuming, require much effort and cost. Therefore, a systematic analysis of determining optimum image resolution is always necessary to tackle these issues. In this study we have analysed micro-CT images of quartz sand grains having similar sizes to find their optimum image resolution that can be used to calculate their shape factors.

SAMPLE PREPARATION AND IMAGE ACQUISITION

We have collected quartz sand from Esperance Beach (33°59'40"S 122°13'57"E) located south of Western Australia. We pour sand grains in a tube of 3mm diameter filled with water. The reason we submerge the grains in water is that the grains will not be dislodged while the tube rotates during image acquisition. We use VersaXRM-500 micro-CT (X-Radia-Zeiss) with an X-ray energy of 80 kV at four different resolutions (Figure 1). Table 1 shows the information on the acquired images of all the resolutions.

Table 1: Image resolution and number of slices acquired and used in the study.

Resolution (voxel edge/ μm)	Number of slices acquired	Number of slices used in the study
0.6528	988	988
1.0231	990	637
1.9628	992	310
3.4348	992	147

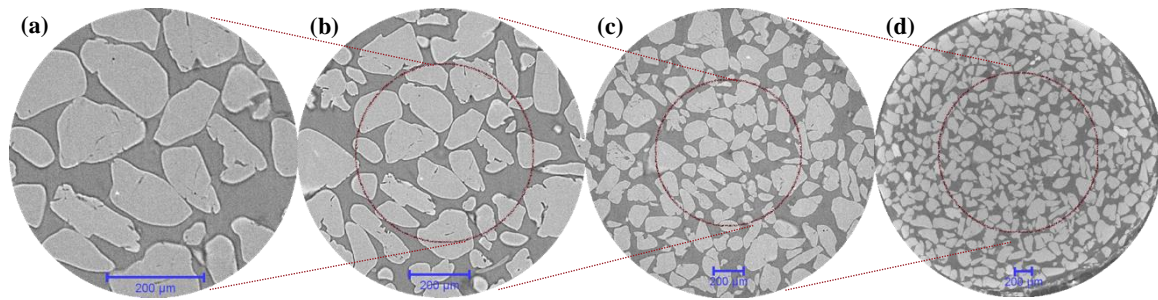


Figure 1: A single slice of image from four resolutions (a) 0.6528 $\mu\text{m}/\text{voxel}$ edge, (b) 1.0231 $\mu\text{m}/\text{voxel}$ edge, (c) 1.9628 $\mu\text{m}/\text{voxel}$ edge and (d) 3.4348 $\mu\text{m}/\text{voxel}$ edge. Red circles show the region of next higher resolution image.

IMAGE PROCESSING

In image processing and calculating morphologic parameters, we use commercial specialized software Avizo 9.2. All the images are very good in quality but still have some noises (Figure 2(a)). To remove those noise, we use *Non-local means filter* (Figure 2(b)) which is a modified version of Buades et al. (2005). To save the computation time I using this filter, instead of using all the voxels of the image at a time, Avizo uses a search window that compares the value of every other voxel inside that window and gives a weighted result. Then we extract the grains from the background by applying a threshold value based on the grey levels of the voxels using *Auto Thresholding* (Figure 2(c)). The selected threshold value is calculated following the algorithms introduced by Otsu (1979). Some of the grains may have holes or artificial void space inside. To fill those voids, we apply *Fill Holes* which follows a sequence of complementing-dilating-complementing of the images where in the end result the grains are filled with voxels belong to the grain (Figure 2(d)). Now we have all the grains separated from the background but they are still attached with their neighbouring grains. To separate the grains from each other, we apply *Separate object* module which follows a high level combination of watershed, distance transform and numerical reconstruction (Figure 2(e)). To get rid of the partial grains that are cut by the image boundary, we use *Border kill* which assigns 0 value to all the voxels of any grain that touches the border voxels of the image (Figure 2(f)). Finally, all the full individual grains get their individual unique identification number or labels after using *Labelling* (Figure 2(g)). We can now call each of the full grains by their unique labels for calculating desired parameters (Figure 2(h)).

Following the above mentioned processing steps, we have got 14 full grains from the image of $(0.6528 \mu\text{m})^3/\text{voxel}$. We extract the same grains from the images of other three resolutions to compare their shape factors.

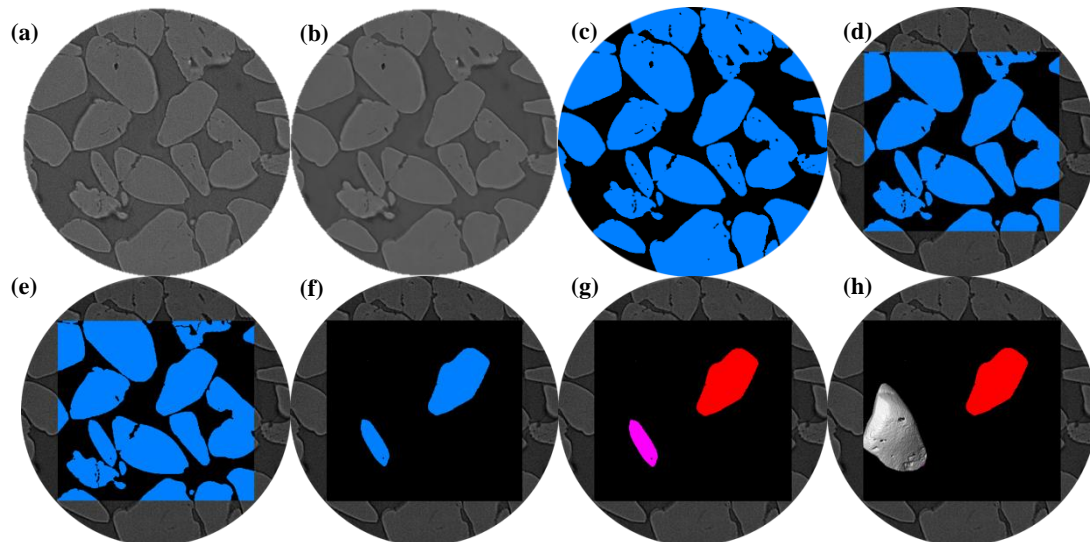


Figure 2: Image processing steps. (a) acquired image, (b) non-local means filtered, (c) grains separated from background, (d) holes enclosed inside the grain filled, (e) grains separated from each other, (f) eliminate partial grains that touch the image border, (g) grains assigned with unique identification number, and (h) extracting single grain for calculating parameters.

SHAPE CHARACTERISTICS

We have calculated a number of attributes from Avizo to define the shape characteristics of the grains. To calculate the size of a grain, we use *equivalent diameter* which is equal to the diameter of a sphere that has same volume of that particular grain (equation 1). The volume of a grain here comes from the total number of voxels multiplied by the image resolution.

$$\text{Equivalent diameter, } EqD = \sqrt[3]{\frac{6 \times \text{Volume}}{\pi}} \quad (1)$$

We calculate the surface area of the grain boundary using Avizo module *Area 3D* which calculates exposed surface area of the boundary voxels using the intercepts connected among those voxels. Sphericity is one of the mostly used shape factor that defines how a particular grain resembles with a perfect sphere. We use the equation from Wadell (1932) which described as the ratio of the surface area of a sphere calculated from the volume of a grain to the surface area of that grain. The range of this sphericity lies between 0 and 1, where 1 is for a perfect sphere.

$$\text{Sphericity, } Sph = \frac{\sqrt[3]{36 \times \pi \times \text{Volume}^2}}{\text{Surface Area}} \quad (2)$$

Roundness defines how angular the corners or edges of a grain is. The roundness we use here is from the ratio of the surface area of a grain to its surface area calculated from the maximum and minimum diameters (equation 3). Higher values represent more rounded grains. Roundness values from this equation can be more than 1 if the grain has intruding voids or burrows at the surface, that cause the surface area of the grain larger.

$$\text{Roundness, } Rnd = \frac{\text{Surface Area}}{4 \times \pi \times \left(\frac{\text{Diameter}_{\text{Max}} + \text{Diameter}_{\text{Min}}}{4} \right)^2} \quad (3)$$

IMPACT OF IMAGE RESOLUTION IN GRAIN SHAPE

Volume of a grain calculated from its total number of voxels shows a little increase in 1.9628 $\mu\text{m}/\text{voxel}$ edge from the lowest resolution of 3.4348 μm (Figure 3(a)). Calculated volume seems to be remain same for most of the grains at the other two higher end resolutions as in 1.9628 $\mu\text{m}/\text{voxel}$ edge. Equivalent diameter of the grains shows a flat trend as it is calculated from the cube root of its volume and a constant (Figure 3(b)). The parameter that mostly affected by the image resolution is the surface area of the grains. Figure 3(c) shows all the grains have an increasing trend of calculated surface area with increasing resolution following a variety of trends for individual grains. Surface areas of grain 3, 6, 5 and 12 have similar gentle increasing trend with increasing resolution whereas later two grains have almost same surface area in all the resolutions. Almost all the grains show same surface areas in higher resolutions of 1.0231 $\mu\text{m}/\text{voxel}$ edge and 0.6528 $\mu\text{m}/\text{voxel}$ edge. Grains 1, 11, 8 and 16 have sharp increasing trend with increasing resolution whereas later two have nearly same surface areas. Grains 4 and 17 have same surface areas and a gentle increasing trend in lower two resolutions but in higher two resolutions, the former one gets more surface area showing a steep rise in 1.0231 $\mu\text{m}/\text{voxel}$ edge and remains almost same in 0.6528 $\mu\text{m}/\text{voxel}$ edge. Grains 7 and 13 also show similar trend with grain 4 which rise abruptly in 1.0231 $\mu\text{m}/\text{voxel}$. Grains 10 and 14 have abrupt rise in middle two resolutions, from 1.0231 $\mu\text{m}/\text{voxel}$ edge to 0.6528 $\mu\text{m}/\text{voxel}$ edge. Lastly, unlike other grains, surface area of Grain 15 does not become stable at higher end resolutions, rather increasing very rapidly.

Pictures of the grains in Table 2 explain the different increasing trends of surface area in individual grains. All the grains have holes and elongated burrow like features. As resolution increases, these features become visible creating more surface area. Depending on the size of these features whether a particular resolution can be able to resolve how much of those, we are observing the different increasing trends. The exceptional trend in Grain 15 is an example where the grain shape and surface features are so complex and rugose that our observed highest resolution might not be enough to resolve all the surface features, hence showing a very steep increasing trend. Surface areas of most of the grains shown in Figure 3(c) tend to be stable at the higher two resolutions. These stable values suggest that, for these grains, resolution below 0.008 voxel/equivalent diameter (1.0231 $\mu\text{m}/\text{voxel}$ edge) would be a perfect choice to characterize the shape factors using the surface area calculated here.

From the previous equations, we can see that sphericity and roundness values are dependent on the surface area, volume and diameters of the grain. As surface area is the only effected parameter and the other two remain same with increasing resolution, both of the shape factors are solely influenced by the former one. Therefore, increasing resolution which means increasing surface area is decreasing sphericity (Figure 4(a)). One the other hand, for the same reason, roundness is increasing with increasing resolution (Figure 4(b)).

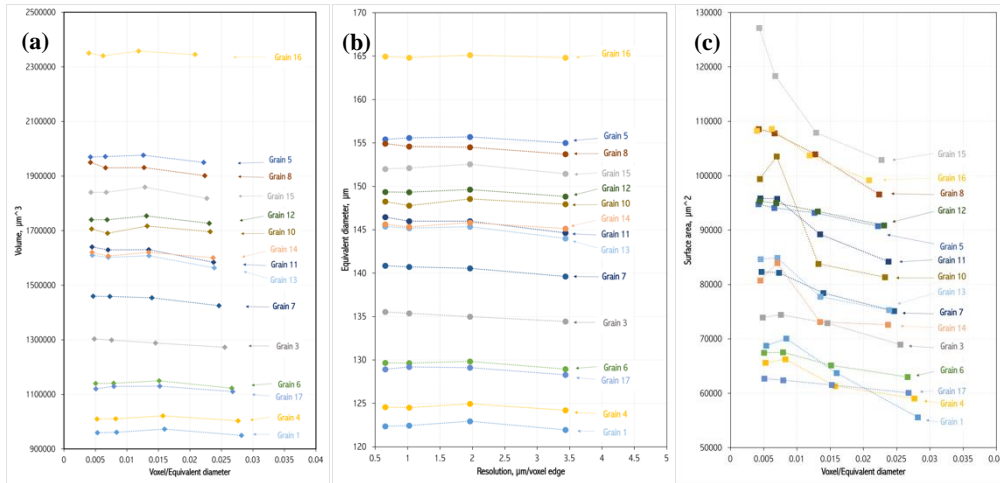


Figure 3: Changes of calculated parameters of the grains with four different image resolutions. (a) Volume, (b) equivalent diameter, and (c) surface area. Images of the grains are shown in the Table 2.

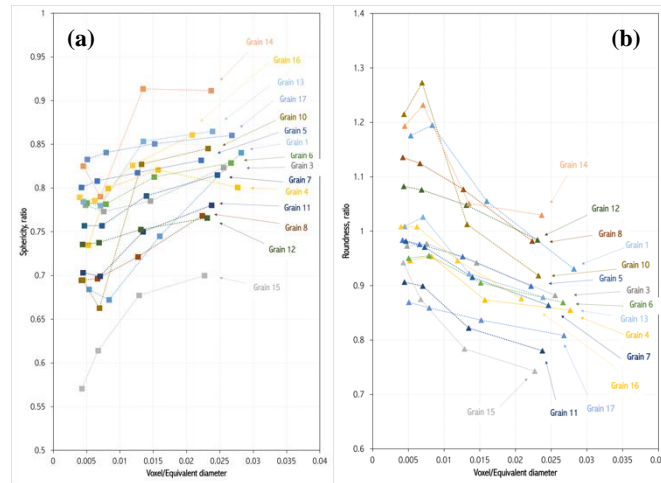


Figure 4: Changes of calculated shape factors of the grains with four different image resolutions. (a) Sphericity, and (b) roundness.

CONCLUSIONS

Surface curvature and rugosities are the key factors that control the calculation of the surface area of the grains. Optimum image resolution of a grain for calculating shape factors mainly dependent on these two factors. The maximum image resolution that can resolve all the undulation of the grain surface should be selected in shape factor calculation keeping in mind about the imaging and computation cost. After studying on these grains, we have found that image resolution of 0.015 voxel/equivalent diameter can be used for volumetric calculations whereas calculations related with the surface area, 0.008 voxel/equivalent diameter should be used.

ACKNOWLEDGMENTS

The work has been supported by the Deep Exploration Technologies Cooperative Research Centre whose activities are funded by the Australian Government's Cooperative Research Centre Programme. This is a DET CRC document. The authors would like to thank the National Geosequestration Laboratory (NGL) for providing access to the X-ray microscope VersaXRM-500 (XRadia-Zeiss Ltd). This work was supported by resources provided by the Pawsey Supercomputing Centre with funding from the Australian Government and the Government of Western Australia. The authors also express their gratitude to ASEG Research Foundation for sponsoring them with Grant (RF16M04). ZA is being supported by Curtin International Postgraduate Research Scholarship and Australian Government Research Training Program Scholarship.

REFERENCES

- Alshibli, K.A., Druckrey, A.M., Al-Raoush, R.I., Weiskittel, T. & Lavrik, N.V. 2015. Quantifying Morphology of Sands Using 3D Imaging. *Journal of Materials in Civil Engineering* **27**, 04014275.
- Bazaikin, Y., Gurevich, B., Iglauer, S., Khachkova, T., Kolyukhin, D., Lebedev, M., Lisitsa, V. & Reshetova, G. 2017. Effect of CT image size and resolution on the accuracy of rock property estimates. *Journal of Geophysical Research: Solid Earth* **122**, 3635-3647.
- Buades, A., Coll, B. & Morel, J. 2005. A non-local algorithm for image denoising. *IEEE CPVR*.
- Cavarretta, I. 2009. The Influence of Particle Characteristics on the Engineering Behaviour of Granular Materials. In: *Dept. of Civil and Environmental Engineering*, Vol. PhD. Imperial College London.
- Cox, M.R. & Budhu, M. 2008. A practical approach to grain shape quantification. *Engineering Geology* **96**, 1-16.
- Dondi, G., Simone, A., Vignali, V. & Manganelli, G. 2012. Discrete Element Modelling of Influences of Grain Shape and Angularity on Performance of Granular Mixes for Asphalts. *Procedia - Social and Behavioral Sciences* **53**, 399-409.
- Druckrey, A.M., Alshibli, K.A. & Al-Raoush, R.I. 2016. 3D characterization of sand particle-to-particle contact and morphology. *Computers and Geotechnics* **74**, 26-35.
- Đuriš, M., Arsenijević, Z., Jaćimovski, D. & Kaluderović Radoičić, T. 2016. Optimal pixel resolution for sand particles size and shape analysis. *Powder Technology* **302**, 177-186.
- Ha Giang, P.H., Van Impe, P., Van Impe, W.F. & Menge, P. Year. Effects of grain size distribution on the initial small strain shear modulus of calcareous sand. Conference Effects of grain size distribution on the initial small strain shear modulus of calcareous sand, Edinburg, UK, 3177-3182.
- Kröner, S. & Doménech Carbó, M.T. 2013. Determination of minimum pixel resolution for shape analysis: Proposal of a new data validation method for computerized images. *Powder Technology* **245**, 297-313.
- Otsu, N. 1979. A Threshold Selection Method from Gray-Level Histograms. *IEEE Trans. Syst. Man Cybern* **9**.
- Santamarina, J.C. & Cho, G.C. Year. Soil behaviour- The role of particle shape. Conference Soil behaviour- The role of particle shape, 604-617.
- Wadell, H. 1932. Shape, and Roundness of Rock Particles. *The Journal of Geology* **40**, 443-451.
- Wildenschild, D. & Sheppard, A.P. 2013. X-ray imaging and analysis techniques for quantifying pore-scale structure and processes in subsurface porous medium systems. *Advances in Water Resources* **51**, 217-246.

Table 2: Calculated parameters of the studied grains with their pictures (not in scale). EqD = Equivalent Diameter, SA = Surface area, Sph = Sphericity, and Rnd = Roundness.

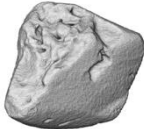
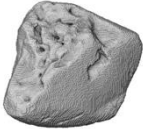

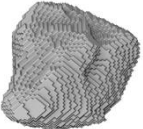
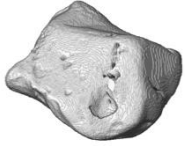
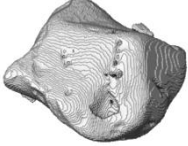
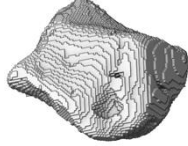
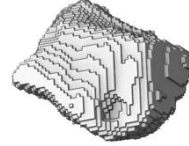
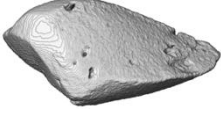
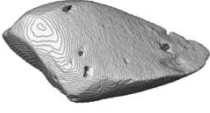
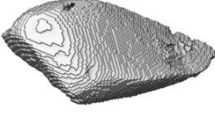
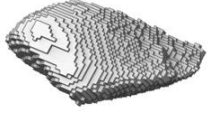



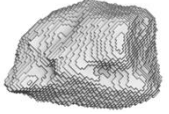
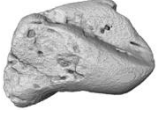
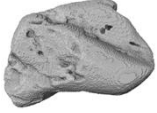

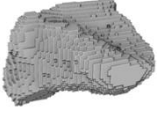
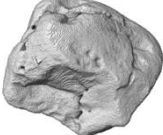
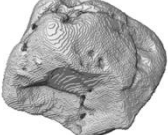
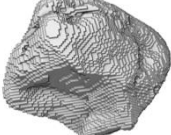
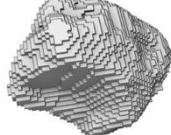
Grain	0.6528 μm /voxel edge	1.0231 μm /voxel edge	1.9628 μm /voxel edge	3.4348 μm /voxel edge
Grain 1				
	EqD: 122.365 SA: 68751.5 Sph: 0.684199 Rnd: 1.17571	EqD: 122.443 SA: 70073.4 Sph: 0.672151 Rnd: 1.19498	EqD: 122.943 SA: 63744.2 Sph: 0.744928 Rnd: 1.05503	EqD: 121.942 SA: 55588.8 Sph: 0.840367 Rnd: 0.930854
Grain 3				
	EqD: 135.527 SA: 73940 Sph: 0.780405 Rnd: 0.972767	EqD:135.381 SA:74456.6 Sph:0.773327 Rnd:0.977012	EqD:134.989 SA:72904 Sph:0.785226 Rnd:0.941599	EqD:134.441 SA:68965.9 Sph:0.823337 Rnd:0.881968
Grain 4				
	EqD: 124.57 SA: 65632.1 Sph:0.742782 Rnd:0.945939	EqD: 124.509 SA:66285.6 Sph:0.734736 Rnd:0.953829	EqD: 124.953 SA:61327.1 Sph:0.799823 Rnd:0.873551	EqD: 124.215 SA:59047.5 Sph:0.820917 Rnd:0.854659
Grain 5				
	EqD:155.415 SA:94778.2 Sph: 0.800616 Rnd:0.983315	EqD:155.572 SA:94083.4 Sph: 0.808164 Rnd:0.975702	EqD:155.706 SA:93173.2 Sph:0.817462 Rnd:0.953217	EqD:155 SA:90731.9 Sph:0.831866 Rnd:0.899095
Grain 6				
	EqD:129.654 SA:67461.8 Sph:0.782819 Rnd:0.950472	EqD:129.633 SA:67531.2 Sph:0.781764 Rnd:0.955184	EqD:129.831 SA:65159.1 Sph:0.812699 Rnd:0.904964	EqD:128.94 SA:63017.5 Sph:0.828829 Rnd:0.868767
Grain 7				
	EqD:140.869 SA:82347.9 Sph:0.757053 Rnd:0.981629	EqD:140.716 SA:82171.8 Sph:0.757028 Rnd:0.970819	EqD:140.547 SA:78447.6 Sph:0.791067 Rnd:0.915278	EqD:139.632 SA:75156.8 Sph:0.814985 Rnd:0.863798

Table 2: Continued

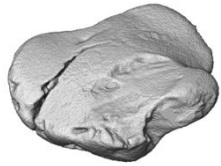
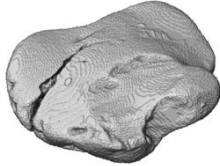
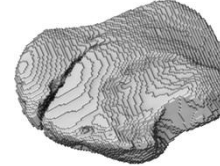
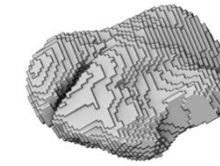
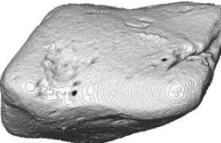
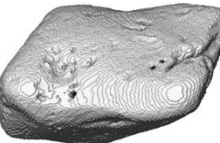
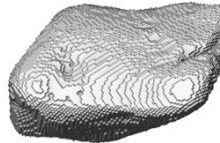
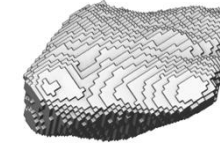


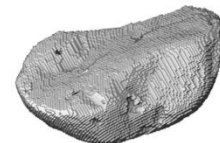
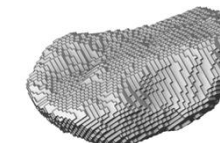
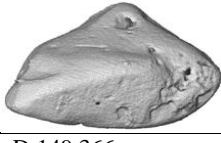
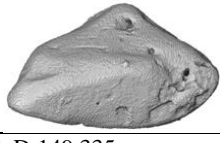
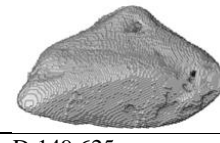
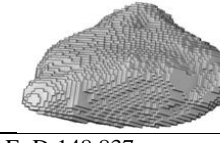


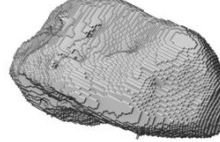
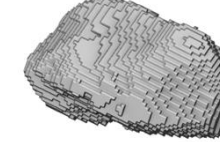

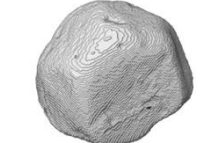
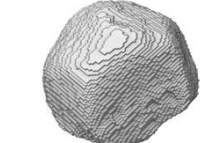
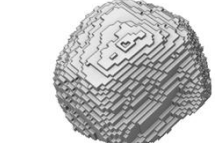
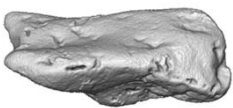
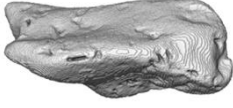

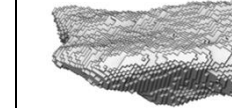
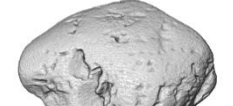
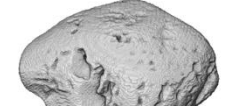

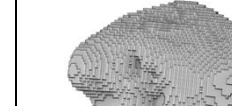


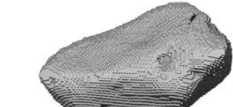
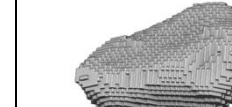
Grain	0.6528 $\mu\text{m}/\text{voxel edge}$	1.0231 $\mu\text{m}/\text{voxel edge}$	1.9628 $\mu\text{m}/\text{voxel edge}$	3.4348 $\mu\text{m}/\text{voxel edge}$
Grain 8				
	EqD:154.913 SA:108553 Sph:0.694519 Rnd:1.13547	EqD:154.583 SA:107802 Sph:0.696373 Rnd:1.12457	EqD:154.495 SA:103958 Sph:0.721308 Rnd:1.07678	EqD:154.495 SA:96579.4 Sph:0.768452 Rnd:0.981625
Grain 10				
	EqD:148.255 SA:99378.9 Sph:0.694822 Rnd:1.21488	EqD:147.794 SA:103548 Sph:0.662709 Rnd:1.27284	EqD:148.56 SA:83818 Sph:0.827214 Rnd:1.01239	EqD:147.96 SA:81359.8 Sph:0.845333 Rnd:0.918214
Grain 11				
	EqD:146.458 SA:95829.5 Sph:0.703201 Rnd:0.906601	EqD:145.988 SA:95754.7 Sph:0.69924 Rnd:0.898959	EqD:145.978 SA:89258 Sph:0.750032 Rnd:0.822104	EqD:144.638 SA:84221 Sph:0.780361 Rnd:0.780356
Grain 12				
	EqD:149.366 SA:95291.2 Sph:0.735528 Rnd:1.08215	EqD:149.335 SA:94991.5 Sph:0.737547 Rnd:1.07591	EqD:149.625 SA:93461.4 Sph:0.752535 Rnd:1.04768	EqD:148.837 SA:90874.1 Sph:0.765832 Rnd:0.984018
Grain 13				
	EqD:145.38 SA:84638.6 Sph:0.784499 Rnd: 1.00879	EqD: 145.187 SA:84919 Sph:0.779829 Rnd:1.02594	EqD:145.344 SA:77755.3 Sph:0.853524 Rnd:0.921983	EqD:143.993 SA:75309.8 Sph:0.864928 Rnd:0.878766
Grain 14				
	EqD:145.637 SA:80740.7 Sph:0.825276 Rnd:1.19312	EqD:145.333 SA:83975.2 Sph:0.790185 Rnd:1.23194	EqD:145.831 SA:73129.6 Sph:0.913598 Rnd:1.05102	EqD:145.121 SA:72595.3 Sph:0.91138 Rnd:1.0295

Table 2: Continued

Grain	0.6528 μm/voxel edge	1.0231 μm/voxel edge	1.9628 μm/voxel edge	3.4348 μm/voxel edge
Grain 15				
	EqD:151.998 SA:127177 Sph:0.570714 Rnd:0.942311	EqD:152.118 SA:118363 Sph:0.614183 Rnd:0.875031	EqD:152.552 SA:107944 Sph:0.677309 Rnd:0.783819	EqD:151.438 SA:102924 Sph:0.700007 Rnd:0.742755
Grain 16				
	EqD:164.96 SA:108293 Sph:0.789419 Rnd:1.00843	EqD:164.816 SA:108613 Sph:0.785715 Rnd:1.00833	EqD:165.127 SA:103699 Sph:0.826055 Rnd:0.945829	EqD:164.832 SA:99158.4 Sph:0.860799 Rnd:0.876115
Grain 17				
	EqD:128.919 SA:62700.7 Sph:0.832743 Rnd:0.869205	EqD:129.205 SA:62385.7 Sph:0.84066 Rnd:0.859221	EqD:129.105 SA:61566.8 Sph:0.850533 Rnd:0.836583	EqD:128.297 SA:60109.8 Sph:0.860271 Rnd:0.808346